

Series Expansion-Based Genetic Inversion of Wireline Logging Data

Norbert Péter Szabó^{1,2} · Mihály Dobróka¹

Received: 24 November 2017 / Accepted: 8 October 2018
© International Association for Mathematical Geosciences 2018

Abstract An evolutionary approach is applied to solve the nonlinear well logging inverse problem. In the framework of the proposed interval inversion method, nuclear, sonic, and laterolog resistivity data measured at an arbitrary depth interval are jointly inverted, where the depth variation of porosity, water saturation, and shale volume is expanded into series using Legendre polynomials as basis functions. In the interval inversion procedure, the series expansion coefficients are estimated by using an adaptive float-encoded genetic algorithm. Since the solution of the inverse problem using traditional linear optimization tools highly depends on the selection of the initial model, a heuristic search is necessary to reduce the initial model dependence of the interval inversion procedure. The genetic inversion strategy used in interval inversion seeks the global extreme of the objective function and provides an estimate of the vertical distribution of petrophysical parameters, even starting the inversion procedure from extremely high distances from the optimum. For a faster computational process, after a couple of thousand generations, the genetic algorithm is replaced by some linear optimization steps. The added advantage of using the Marquardt algorithm is the possibility to characterize the accuracy of the series expansion coefficients and derived petrophysical properties. A Hungarian oil field example demonstrates the feasibility and stability of the improved interval inversion method. As a significance, the genetic inversion method does not require prior knowledge or strong restrictions on the

✉ Norbert Péter Szabó
norbert.szabo.phd@gmail.com
Mihály Dobróka
dobroka@uni-miskolc.hu

¹ Department of Geophysics, University of Miskolc, Miskolc-Egyetemváros 3515, Hungary

² MTA-ME Geoenvironment Research Group, University of Miskolc, Miskolc-Egyetemváros 3515, Hungary

20 values of petrophysical properties and gives highly reliable estimation results practi-
21 cally independent of the initial model and core information.

22 **Keywords** Float-encoded genetic algorithm · Interval inversion · Series expansion ·
23 Petrophysical parameter · Hungarian oil fields

24 1 Introduction

25 In oil field petrophysics, well logging inversion has been an integral part of computer-
26 processed log analysis for more than three decades, the traditional method of which
27 is based on the linearization of the functional relation between the measurements
28 and the estimated petrophysical model (Mayer and Sibbit 1980). This linear opti-
29 mization approach is widely used in formation evaluation, which offers a fast and
30 satisfactory solution when one has appropriate prior information on the petrophysi-
31 cal characteristics of the hydrocarbon reservoir. The theory and geophysical aspects
32 of linear inversion methods are detailed in Menke (1984) and Tarantola (2005). The
33 strongest limitation of the gradient-based search techniques is that they usually find
34 a local minimum of the objective function in the near vicinity of the initial model.
35 To improve the performance of inverse modeling in terms of optimization, Sen and
36 Stoffa (1995) recommended the use of global optimization methods such as simulated
37 annealing and genetic algorithm. Since these optimization techniques do not require
38 the calculation of the Jacobi matrix and look for the solution not only in the direction
39 of the local minimum, they can wander freely in the parameter space and try many
40 possible solutions. During their random search, not only the best models but also
41 some of those with worse data misfit are temporarily accepted to avoid the localities
42 and ambiguous solutions. Global optimization methods are able to solve constrained
43 and strongly nonlinear inverse problems with high efficiency and adaptability, as they
44 are capable of finding better solutions than local-optimization methods without any
45 curvature information of the misfit function and a good starting model (Sambridge
46 and Drijkoningen 1992; Mundim et al. 1998; Tlas and Asfahani 2008; Yang 2013;
47 Toushmalani 2013). However, the global inversion techniques are computationally
48 intensive; thus, they can be used most preferably in case of quickly computable forward
49 problems and relatively small number of model parameters. For these reasons, their
50 application provides several perspectives to well logging inversion (Szűcs and Civan
51 1996; Szabó 2004; Dobróka and Szabó 2012; Malkoti et al. 2017). The rapid devel-
52 opment of computational power and capacity allows the ever-expanding use of global
53 optimization techniques and similar metaheuristic approaches for solving complex
54 optimization problems in petroleum geosciences (Cranganu et al. 2015). In well log
55 analysis, for example, they have already been used in finite element modeling-assisted
56 three-dimensional inversion of DC resistivity measurements (Gajda-Zagórska et al.
57 2015), in reservoir characterization using the combination of genetic algorithm and
58 particle swarm optimization (Ali Ahmadi et al. 2013), in neural-network prediction
59 of wireline logs from seismic attributes (Dorrington and Link 2004), in estimating the
60 seismic velocities from well logs (Aleardi 2015), and in a genetic algorithm-assisted

61 factor analysis to estimate the shale volume and permeability in hydrocarbon reservoirs
62 (Szabó and Dobróka 2018).

63 Open-hole logging data are traditionally processed in separated inversion proce-
64 dures at different depths. The inverse problem is solved in a given depth by minimizing
65 the misfit between the predicted and observed data normalized by the data variances
66 using the weighted least squares method (Mayer and Sibbit 1980). Several applications
67 for this local inversion methodology have been published; for example, in the analysis
68 of oil field well logs (Ball et al. 1987; Narayan and Yadav 2006; Woznicka et al. 2009)
69 and direct-push logging data (Drahos 2005). Having barely more data than unknowns
70 in the investigated depth, a set of marginally overdetermined inverse problems is to
71 be run along the borehole. The narrow overdetermination sets a limit to the number of
72 unknowns to be extracted and makes the inversion procedure highly sensitive to data
73 noise. Moreover, the local inversion approach does not allow the estimation of layer
74 thicknesses because they are not included explicitly in the local response functions,
75 although this information is inherent in the entire well-logging data set. The marginal
76 overdetermination of the local inverse problem is not favorable to the estimation of
77 zone parameters. These parameters are normally fixed for the inversion process, which
78 causes further uncertainty in the inverse problem solution.

79 Dobróka et al. (2016) suggested to increase the overdetermination (data-to-
80 unknowns) ratio by using a series expansion-based inversion methodology to improve
81 the quality of well logging inversion results. In the so-called interval inversion proce-
82 dure, all data collected at a depth interval are jointly inverted to estimate the series
83 expansion coefficients far less in number than data, which describes the vertical varia-
84 tion of petrophysical properties. The remarkably high overdetermination of the inverse
85 problem significantly increases the noise suppression capability of the interval inver-
86 sion method, as well as the accuracy and reliability of the inversion result. Moreover,
87 the interval inversion procedure allows the automated estimation of such unknowns
88 that have not been estimated by inversion; for instance, Archie's textural parameters,
89 the physical properties of rock-forming minerals and fluids included in the sonde
90 response functions (Dobróka and Szabó 2011), as well as the vertical coordinates
91 of layer boundaries and their horizontal variation between the wells (Dobróka et al.
92 2009; Dobróka and Szabó 2012). Other statistical approaches different from the inter-
93 val inversion method, which uses depth-dependent basis functions to describe the
94 variation of petrophysical properties, are also applied for a more advanced analysis of
95 well logs. The advantages of the introduction of a vertical continuity model in facies
96 classification was shown by Eidsvik et al. (2004) and Lindberg and Grana (2015).
97 They suggested modeling the continuous well-logging measurements as the result of
98 a hidden Markov chain model for improved classification of hydrocarbon formations.

99 Similar to other inversion methods, the performance of the interval inversion proce-
100 dure highly depends on the applied model discretization scheme. When choosing
101 the number of unknowns, a compromise has to be made between the stability of the
102 inversion procedure and the accuracy of the estimation results. In the first applications
103 of interval inversion, the combination of Heaviside step (basis) functions were used
104 to describe the petrophysical properties in sequential homogeneous layers (Dobróka
105 et al. 2012). Since this was the case with the smallest possible number of unknowns,
106 this approach resulted in a highly stable interval inversion procedure, but also a rough

107 approximation of the variation of petrophysical properties along a borehole. In recent
108 applications, orthogonal sets of polynomials have been selected as basis functions
109 to model inhomogeneous formations (Dobróka et al. 2016; Szabó et al. 2018). The
110 latter approach has proven to give higher spatial resolution of the petrophysical model
111 and less correlated model parameters than using other basis functions; for instance,
112 power functions or other non-orthogonal polynomials. However, it has been recently
113 experienced that, by a large number of expansion coefficients as unknown, in certain
114 cases, the stability of the inversion procedure is reduced and this phenomenon is highly
115 dependent on the selection of the starting model. Although the inversion procedure can
116 be numerically stabilized by regularization, it may still either trap in a local minimum
117 or become divergent and continue to be sensitive to the initial model.

118 To avoid this difficulty, the interval inversion method is further developed by using a
119 float-encoded genetic algorithm (FGA) suggested by Michalewicz (1992). This adap-
120 tive genetic inversion approach is used to determine the petrophysical parameters
121 expanded into series using Legendre polynomials. In order to accelerate the time-
122 consuming search for the global optimum, the genetic inversion process is coupled
123 by some linear optimization steps using the damped least squares (DLSQ) method
124 (Marquardt 1959). The sequential application of global and linear optimization tech-
125 niques has been effectively used previously; for instance, in the joint inversion of
126 geoelectric and seismic data (Chundururu et al. 1997). In the initialization phase of the
127 genetic (interval) inversion procedure, the individuals of the initial population are gen-
128 erated randomly from a wide value range of model parameters (i.e., series expansion
129 coefficients). The heuristic search improves the actual population of models, while it
130 effectively avoids the local extrema of the objective function, defined as a norm of
131 the difference between the measured and theoretical data vectors. At the end of the
132 genetic process, a first approximation of the petrophysical parameters derived from
133 the expansion coefficients is given, even when starting the inversion procedure from
134 extremely high distances from the global optimum. After a requisite number of gener-
135 ations, the FGA is replaced by the DLSQ algorithm, in which the vertical distribution
136 of petrophysical parameters is further refined and the data misfit is quickly reduced
137 to an optimal level. A Hungarian case study including the petrophysical evaluation
138 of an unconsolidated hydrocarbon formation shows that the above suggested genetic
139 inversion method is able to find the optimal values of series expansion coefficients and
140 the related petrophysical parameters in a stable inversion procedure.

141 2 Theory and Methods

142 2.1 Forward Modeling

143 The interval inversion method allows the estimation of porosity, water saturation, shale
144 content, and matrix volume in clastic hydrocarbon formations. In each generation of
145 the genetic inversion procedure, theoretical well logs are calculated and compared to
146 real data observed along the borehole. The synthetic logs are generated in the forward
147 modeling procedure by assuming a known petrophysical model. For this purpose, the

148 following sonde response functions are used for unconsolidated shaly-sand formations
149 (Wyllie et al. 1956; Alberty and Hashmy 1984; Schlumberger 1989)

$$150 \quad \rho_b = \Phi [\rho_{mf} - 1.07 (1 - S_{x0}) (\alpha_0 \rho_{mf} - 1.24 \rho_{hc})] + V_{sh} \rho_{sh} + V_{sd} \rho_{sd}, \quad (1)$$

$$151 \quad GR = \rho_b^{-1} (V_{sh} GR_{sh} \rho_{sh} + V_{sd} GR_{sd} \rho_{sd}), \quad (2)$$

$$152 \quad \Phi_N = \Phi \left\{ \begin{aligned} &\Phi_{N,mf} - (1 - S_{x0}) C_{cor} - 2\Phi (1 - S_{x0}) S_{hf} (1 - 2.2\rho_{hc}) \\ &\cdot [1 - (1 - S_{x0}) (1 - 2.2\rho_{hc})] \end{aligned} \right\}$$

$$153 \quad + V_{sh} \Phi_{N,sh} + V_{sd} \Phi_{N,sd}, \quad (3)$$

$$153 \quad \Delta t = \Phi [\Delta t_{mf} S_{x0} + (1 - S_{x0}) \Delta t_{hc}] c_p + V_{sh} \Delta t_{sh} + V_{sd} \Delta t_{sd}, \quad (4)$$

$$154 \quad R_t = \left[\frac{\Phi^m S_w^n}{a R_w (1 - V_{sh})} + \frac{V_{sh} S_w}{R_{sh}} \right]^{-1}, \quad (5)$$

156 where the notations of calculated well log types are summarized in Table 1. The com-
157 mon parameters in Eqs. (1)–(5) are the volumetric fractions of the rock's fluid and solid
158 constituents, such as shale-free porosity (Φ), shale volume (V_{sh}), sand volume (V_{sd}),
159 and water saturation in the invaded zone (S_{x0}) and that of the virgin zone (S_w). In the
160 framework of the traditional local (depth-by-depth) inversion, the physical properties
161 of mud filtrate (mf), hydrocarbon (hc), shale (sh), and sand (sd) are treated as constants
162 to solve a marginally overdetermined (local) inverse problem (Table 1). The textural
163 parameters in Eq. (5), namely, the cementation exponent (m), saturation exponent (n),
164 and tortuosity factor (a), are also fixed in local inversion (Archie 1942). These zone
165 parameters can be set by crossplot techniques, core information, or from the literature.
166 Some constants in Eqs. (1) and (3) come from empirical considerations used in the
167 oil industry. Since these physical parameters do not vary as fast as the volumetric
168 properties in a hydrocarbon formation or a zone, they are necessarily fixed for the
169 interval inversion experiments. In this study, the genetic (interval) inversion method
170 is suggested to determine only the volumetric properties; however, the highly overde-
171 termined interval inversion method allows the estimation of some zone parameters
172 simultaneously with the volumetric properties in an automated inversion procedure
173 (Dobróka and Szabó 2011). The interval inversion framework also gives a possibility
174 for the integration of new data types, the response functions of which can be freely
175 chosen. The solution of the forward problem can be necessarily further improved, pri-
176 marily in the case of a nonlinear resistivity response equation, with the more accurate
177 account of borehole effects and mud invasion (Galsa et al. 2016; Jarzyna et al. 2016;
178 Szijártó et al. 2017).

179 2.2 Genetic Inversion Approach

180 The evolutionary technique incorporating a large group of soft computing methods
181 was first proposed by Holland (1975). The genetic algorithm is a highly adaptive
182 and efficient optimization tool, which employs the mechanism of natural selection.
183 In its meta-heuristic searching process, a population of models as artificial individu-
184 als is iteratively improved generation by generation. The quality of an individual is

Table 1 Zone parameters chosen for genetic interval inversion of wireline logs measured in well H

Open-hole log	Zone parameter	Symbol	Constant	Unit
Gamma ray intensity (GR)	Sand	GR_{sd}	13	API
	Shale	GR_{sh}	160	API
Density (ρ_b)	Sand	ρ_{sd}	2.6	g/cm^3
	Shale	ρ_{sh}	2.47	g/cm^3
	Mud filtrate	ρ_{mf}	1.2	g/cm^3
	Gas	ρ_{hc}	0.135	g/cm^3
	Mud filtrate coefficient	α	1.11	–
Neutron porosity (Φ_N)	Sand	$\Phi_{N,sd}$	– 0.035	v/v
	Shale	$\Phi_{N,sh}$	0.3	v/v
	Mud filtrate	$\Phi_{N,mf}$	1	v/v
	Mud filtrate coefficient	C_{cor}	0.69	–
	Residual hydrocarbon coefficient	S_{hrf}	1.17	–
Acoustic interval time (Δt)	Sand	Δt_{sd}	56	$\mu s/ft$
	Shale	Δt_{sh}	108	$\mu s/ft$
	Mud filtrate	Δt_{mf}	188	$\mu s/ft$
	Gas	Δt_{hc}	211	$\mu s/ft$
	Compaction factor	c_p	1.08	–
True resistivity (R_t)	Shale	R_{sh}	1.0	Ωm
	Pore water	R_w	0.4	Ωm
	Mud filtrate	R_{mf}	0.28	Ωm
	Cementation exponent	m	1.4	–
	Saturation exponent	n	1.7	–
	Tortuosity factor	a	0.9	–

185 characterized by a fitness function specifying its survival capability. According to
 186 Darwin's theory, the fittest individuals are more likely to survive and reproduce, while
 187 others disappear from the population. The individuals are represented by chromo-
 188 somes, the elements of which, called genes, are randomly exchanged and modified
 189 during the genetic computation process. The FGA is known as one of the most effi-
 190 cient global optimization methods, which applies real-valued operations directly on
 191 the genes for the best resolution and computational performance (Michalewicz 1992).

192 In this study, an evolutionary computation strategy is applied to solve the nonlinear
 193 problem of interval inversion. In the local inversion approach as a traditional method
 194 of well log analysis, the data set of a given depth is processed to estimate the petro-
 195 physical properties to the same depth in a quick linearized inversion procedure. In the
 196 interval inversion procedure, all data measured over a depth interval of arbitrary length

197 is simultaneously inverted to estimate the vertical distribution of petrophysical param-
 198 eters. For this purpose, the local response functions are extended to a depth-dependent
 199 form as

$$d_k^{(\text{cal})}(z) = g_k(m_1(z), \dots, m_i(z), \dots, m_M(z)), \quad (6)$$

202 where m_i is the i th petrophysical property (M is the total number of petrophysical
 203 parameters) and g_k represents the response function of the k th sonde ($k = 1, 2, \dots, K$,
 204 where K is the number of applied logging tools). The zone parameters are assumed
 205 constant (since their estimation is not the subject of the present study). Dobróka et al.
 206 (2016) introduced a series expansion technique for the discretization of model param-
 207 eters, where the i th petrophysical parameter, such as porosity or shale volume, is
 208 approximated as

$$m_i(z) = \sum_{q=1}^{Q^{(i)}} B_q^{(i)} P_{q-1}(z), \quad (7)$$

211 where B_q is the q th expansion coefficient, $P_{q-1}(z) = P_l(z) = (2^l l!)^{-1} \frac{d^l}{dz^l} (z^2 - 1)^l$
 212 is the l th degree Legendre polynomial as the basis function, and $Q^{(i)}$ is the number
 213 of expansion coefficients for describing the i th model parameter along the processed
 214 interval ($i = 1, 2, \dots, M$). The Legendre polynomials form an orthonormal set of func-
 215 tions over the interval $[-1, 1]$, where the depth range of well logging measurements
 216 are linearly scaled. The Legendre polynomials up to the sextic degree are plotted in
 217 Fig. 1. In geophysical inversion, the problem of ambiguity primarily arises from the
 218 high correlation between the model parameters. Since there is no attachment between
 219 the Legendre polynomials of different orders, a relatively weak correlation is indicated
 220 between the estimated model parameters. This approach results in a unique solution
 221 and stable inversion procedure. Hence, the interval inversion method applying Legen-
 222 dre polynomials gives more accurate estimates to the series expansion coefficients than
 223 by using power functions or other non-orthogonal polynomials. The added advantage
 224 of implementing Eq. (7) is that the petrophysical model can be described by a signif-
 225 icantly smaller number of expansion coefficients than data, which can be extracted in
 226 a greatly overdetermined inversion procedure.

227 Consider the combination of Eqs. (6) and (7), which expresses the calculation of
 228 the k th log type with the series expansion coefficients

$$d_k^{(\text{cal})}(z) = g_k(B_1^{(1)}, \dots, B_{Q^{(1)}}^{(1)}, \dots, B_1^{(M)}, \dots, B_{Q^{(M)}}^{(M)}, z). \quad (8)$$

231 The expansion coefficients forming independent variables of the
 232 above response function are collected into the column vector $\mathbf{B} =$
 233 $[B_1^{(1)}, \dots, B_{Q^{(1)}}^{(1)}, \dots, B_1^{(M)}, \dots, B_{Q^{(M)}}^{(M)}]^T$, which are the unknowns of the inverse
 234 problem. In the genetic inversion procedure, the population of individuals is formed by
 235 a number of series expansion coefficient vectors, which represent possible solutions
 236 to the inverse problem. First, one must integrate all well log types measured over the

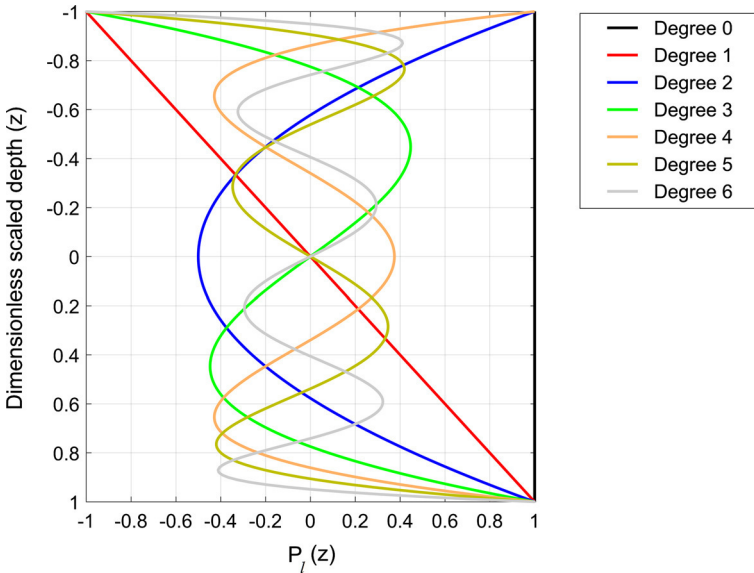


Fig. 1 Legendre polynomials of the l th degree ($l = 0, 1, \dots, 6$) as depth functions plotted in the range $[-1, 1]$

237 processing interval into the data matrix $\mathbf{D}^{(\text{obs})}$, the k th column of which includes all
 238 data of the k th observed quantity along the selected depth interval of the borehole.
 239 The matrix of theoretical well logging data is of equal size and calculated by Eq. (8).
 240 The misfit between the measured and calculated data is related to the fitness function

$$241 \quad F(\mathbf{B}^{(s)}) = - \left[(NK)^{-1} \sum_{n=1}^N \sum_{k=1}^K \left(\frac{D_{nk}^{(\text{obs})} - g_k(\mathbf{B}^{(s)}, z_n)}{D_{nk}^{(\text{obs})}} \right)^2 \right]^{1/2}, \quad (9)$$

242

243 where D_{nk} is the k th data measured in the n th depth and $\mathbf{B}^{(s)}$ is the s th series expansion
 244 vector ($s = 1, 2, \dots, S$, where S is the population size). For maximizing the average
 245 fitness of the population, real genetic operations such as selection, crossover, and
 246 mutation are repeatedly applied on the individuals in consecutive generations (Houck
 247 et al. 1995).

248 At the beginning of the genetic inversion procedure, the fittest individuals are
 249 selected for reproduction by using the normalized geometric ranking operator. At
 250 first, the individuals are sorted by their fitness values calculated by Eq. (9). The rank
 251 of the fittest model is 1, while that of the worst adaptable one is S . The probability of
 252 selecting the i th expansion coefficient vector is expressed by

$$253 \quad P(\mathbf{B}^{(i)}) = \frac{P_b}{1 - (1 - P_b)^S} (1 - P_b)^{r_i - 1}, \quad (10)$$

254

255 where r_i is the rank of the i th expansion coefficient vector and P_b is the probability
 256 of selecting the best model. The cumulative probability of the ranked population is

257 $C_i = \sum_{t=1}^i P(\mathbf{B}^{(t)})$. If the condition fulfils $C_{i-1} < \beta \leq C_i$, the i th chromosome of
 258 series expansion coefficients is copied into the new population, where β is a random
 259 number from the uniform density on $[0, 1]$. In the next step, a pair of individuals $\mathbf{B}^{(1)}$
 260 and $\mathbf{B}^{(2)}$ are chosen from the selected population to exchange some genes between
 261 them. The crossover operator normally cuts the chromosomes at one or more crossover
 262 points and swaps the expansion coefficients to the right of them. In this study, the
 263 heuristic crossover operation is applied that extrapolates two models as

$$\begin{aligned} \mathbf{B}^{*(1)} &= \mathbf{B}^{(1)} + \gamma (\mathbf{B}^{(1)} - \mathbf{B}^{(2)}), \\ \mathbf{B}^{*(2)} &= \mathbf{B}^{(1)}, \end{aligned} \quad (11)$$

266 where γ is a random number generated from $U(0, 1)$. The condition of using Eq. (11)
 267 is that the fitness of $\mathbf{B}^{(1)}$ is higher than that of $\mathbf{B}^{(2)}$. If any value of $\mathbf{B}^{*(1)}$ is out of
 268 range, the generation of γ is to be repeated and Eq. (11) is recalculated. After some
 269 hundreds of failures, the values of expansion coefficients are changed to the old ones.
 270 The last genetic operator is uniform mutation, where the individual $\mathbf{B}^{*(1)}$ is selected
 271 and its v th expansion coefficient is substituted with the random number η chosen from
 272 its possible range

$$\mathbf{B}^{**{(1)}} = \begin{cases} \eta, & \text{if } v = h \\ B_v^{*(1)}, & \text{otherwise} \end{cases}, \quad (12)$$

275 where $\mathbf{B}^{**{(1)}}$ is the mutated vector of series expansion coefficients. Equations (10)–(12)
 276 are applied repeatedly in successive generations until a termination criterion is met. In
 277 the last generation, the expansion coefficient vector with maximum fitness is regarded
 278 as the solution. At the end of the inversion procedure, the petrophysical properties are
 279 extracted from the expansion coefficients using Eq. (7) and the depth coordinates are
 280 rescaled to their original range.

281 2.3 Quality Check of the Inversion Result

282 The development of convergence of the interval inversion procedure can be signif-
 283 icantly accelerated by switching the FGA around the global optimum to linearized
 284 optimization. In the last optimization phase, not just the estimation of the petrophys-
 285 ical model is finalized but also the Jacobi matrix is calculated, holding information
 286 on the accuracy of the model parameters. The calculation of the estimation error of
 287 petrophysical parameters would take an unreasonably high computational time when
 288 executing the genetic inversion procedure several times. Instead of doing so, the DLSQ
 289 method is used as a post-processing calculation method in the interval inversion work-
 290 flow.

291 Menke (1984) showed that the model covariance matrix estimated by a linearized
 292 inversion method is directly proportional to the data covariance matrix including the

293 uncertainties of observed data. This can be written for the series expansion coefficients
294 as

$$295 \quad \text{cov}\mathbf{B} = \mathbf{G}^{-g} \text{cov}\mathbf{d}^{(\text{obs})} (\mathbf{G}^{-g})^T, \quad (13)$$

297 where $\mathbf{d}^{(\text{obs})}$ denotes the observed data vector of the linear inverse problem and \mathbf{G}^{-g} is
298 the general inverse matrix of the DLSQ method (Marquardt 1959). The linearization of
299 the nonlinear inverse problem produces an approximated uncertainty appraisal. To cast
300 the genetic algorithm inversion in a solid probabilistic framework, the neighborhood
301 algorithm (Sambridge 1999) or a hybrid genetic algorithm-Gibbs sampler approach
302 (Aleari and Mazzotti 2017), for instance, can be suggested. The linear approach of
303 Menke (1984) is a standard method of uncertainty analysis in the oil field practice,
304 based upon which a comparative study can be made between the traditional local
305 inversion method and the suggested interval inversion procedure. The genetic algo-
306 rithm phase of the interval inversion procedure is very time-consuming. In this study,
307 global optimization is used for setting a proper initial model for the subsequent linear
308 phase, in which the estimation errors can be calculated relatively quickly. By knowing
309 the optimal values of the expansion coefficients, Eq. (7) is used to derive the depth
310 function of petrophysical properties. The estimation error of petrophysical parameters
311 derived from Eq. (13) requires the propagation of errors to be taken into account.
312 Dobróka et al. (2016) introduced the depth-dependent model covariance matrix for
313 the petrophysical parameters as

$$314 \quad [\text{cov}\mathbf{m}(z)]_{ij} = \sum_{w=1}^{Q^{(i)}} \sum_{t=1}^{Q^{(j)}} P_{w-1}(z) (\text{cov}\mathbf{B})_{uv} P_{t-1}(z), \quad (14)$$

316 where indices i and j run from 1 to M and indices u and v are $u = w + Q^{(1)} +$
317 $Q^{(2)} + \dots + Q^{(i-1)}$ and $v = t + Q^{(1)} + Q^{(2)} + \dots + Q^{(j-1)}$. The main diagonal
318 of the model covariance matrix includes the variances of the petrophysical quanti-
319 ties. The estimation error of the i th petrophysical parameter is derived from Eq. (14)
320 as $\sigma[m_i(z)] = [\text{cov}\mathbf{m}_i(z)]^{1/2}$. It can be mentioned that, in case of asymmetric
321 uncertainty ranges of observed variables, one can derive the upper and lower bound-
322 aries of the error intervals of model parameters based on the above methodology
323 (Baker Atlas 1996). As another quality check parameter, the correlation coefficient
324 between the i th and j th petrophysical parameters is calculated as $[\text{corr } \mathbf{m}(z)]_{ij} =$
325 $[\text{cov } \mathbf{m}(z)]_{ij} \sigma[m_i(z)]^{-1} \sigma[m_j(z)]^{-1}$, which characterizes the reliability of the esti-
326 mated model parameters for the entire processing interval. One can introduce the mean
327 spread as a scalar for measuring the average correlation

$$328 \quad R(\mathbf{m}) = \left\{ [M(M-1)]^{-1} \sum_{i=1}^M \sum_{j=1}^M [([\text{cov } \mathbf{m}(z)]_{ij} - \delta_{ij})^2] \right\}^{1/2}, \quad (15)$$

330 where δ denotes the Kronecker symbol (Menke 1984). From the point of view of the
331 inversion procedure, a solution is unreliable when the estimated parameters strongly

332 correlate. In that very case, model parameters are prevented from changing inde-
 333 pendently during the inversion process. Only poorly correlated parameters can be
 334 determined uniquely by inverse modeling referring to a reliable solution. As a third
 335 quantity, the relative data distance measures the overall misfit between the measured
 336 and calculated data matrices

$$337 \quad D_d = \left[(NK)^{-1} \sum_{n=1}^N \sum_{k=1}^K \left(\frac{D_{nk}^{(\text{obs})} - D_{nk}^{(\text{calc})}}{D_{nk}^{(\text{obs})}} \right)^2 \right]^{1/2} \times 100 (\%), \quad (16)$$

339 which takes into account that the observed well logging parameters are of different
 340 magnitudes and dimensional units.

341 3 Results and Interpretation

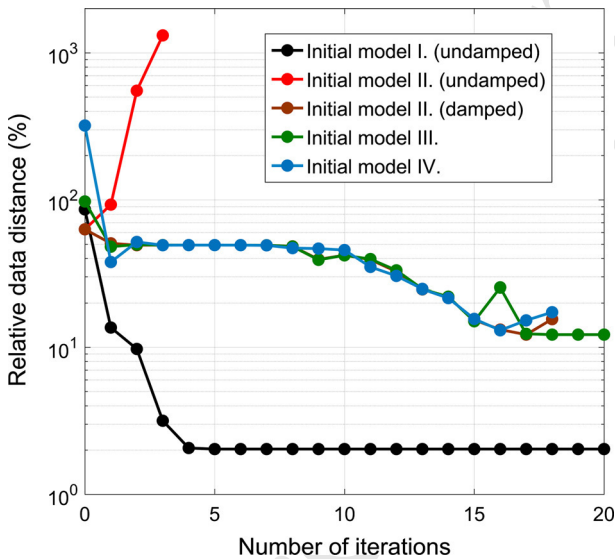
342 3.1 Limitation of Linearized Optimization

343 As a preliminary numerical experiment, the Marquardt algorithm-based (linearized)
 344 interval inversion procedure is tested using a well logging data set measured in a
 345 Hungarian hydrocarbon exploratory borehole (well H). The formation investigated
 346 is composed of unconsolidated gas-bearing shaly-sand reservoirs of Pliocene age.
 347 The natural gamma ray intensity, density, neutron porosity, acoustic traveltime, and
 348 true resistivity logs are simultaneously inverted to estimate the expansion coefficients
 349 describing the porosity, invaded and virgin zone water saturation, and shale volume.
 350 The sand volume is calculated from the well-known material balance equation $\Phi +$
 351 $V_{\text{sh}} + V_{\text{sd}} = 1$. The actual values of zone parameters set in Eqs. (1)–(5) are given in
 352 Table 1. By a sampling distance of 0.1 m, $N = 194$ depth points, and $K = 5$ log types,
 353 970 data are jointly inverted.

354 The petrophysical properties are discretized according to Eq. (7). Legendre poly-
 355 nomials of degree 44 as basis functions are used for describing each petrophysical
 356 parameter. Thus, the total number of unknowns is $Q^* = 180$ (since 45 expansion coef-
 357 ficients are necessary for a petrophysical parameter) and the data-to-unknowns ratio is
 358 5.4 (it is only 1.25 for local inversion). The interval inversion procedure is run by using
 359 different starting models (Table 2). The initial values of the expansion coefficients of
 360 the Legendre polynomials of zero degree are chosen differently for each model. The
 361 expansion coefficient B_1 can be identified as the constant value of the relevant petro-
 362 physical parameter in the processed (equivalent homogeneous) depth interval. The
 363 coefficients of the higher degree basis functions are set to zero. All inversion runs
 364 over 20 iterations are plotted in Fig. 2. It is shown that the inversion process is highly
 365 stable, when model I is used (randomly) as the initial model. By applying Eq. (16),
 366 the relative data distance is calculated on the starting model as $D_{d,0} = 86\%$, which
 367 is continuously decreased to $D_d = 2\%$. Let just one parameter of the initial model
 368 change; for example, the value of shale volume is increased by 0.1. For the new model
 369 (model II), the development of convergence fails even when introducing a non-zero
 370 damping factor (ε). Data predicted on models III and IV fall the farthest from the

Table 2 Starting models used for linearized interval inversion of wireline logs observed in well H

Model no.	$B_1^{(\Phi)}$	$B_1^{(S_w)}$	$B_1^{(V_{sh})}$	$B_1^{(S_{x0})}$	ε	$D_{d,0}$ (%)	D_d (%)
I	0.20	0.40	0.15	0.80	0	86	2.05
II	0.20	0.40	0.25	0.80	0	63	Divergent
					1.0		Divergent
III	0.10	0.50	0.20	0.70	1.0	97	12.20
IV	0.20	0.20	0.10	0.50	1.0	320	Divergent

**Fig. 2** Data distance versus iteration step curves obtained by linearized interval inversion of well logs using different starting models. The parameters of initial models I–IV are given in Table 2

371 observations (see data distances in Table 2). Despite regularization, they do not give
 372 an optimal solution. Although in the case of almost 100% data distance the application
 373 of model III leads to a convergent solution, the search is obviously trapped in a local
 374 minimum of the objective function, Eq. (9). Model IV with an extremely high data
 375 distance represents an ill-conditioned linear inverse problem (caused by a near-zero
 376 determinant of the inverted matrix), which does not give interpretable results. It is con-
 377 cluded that the success of the linear optimization-based interval inversion procedure
 378 critically depends on the selection of the initial model. Inappropriately chosen initial
 379 models lead to a divergent or not an optimal solution, which can be assisted by the use
 380 of genetic inversion.

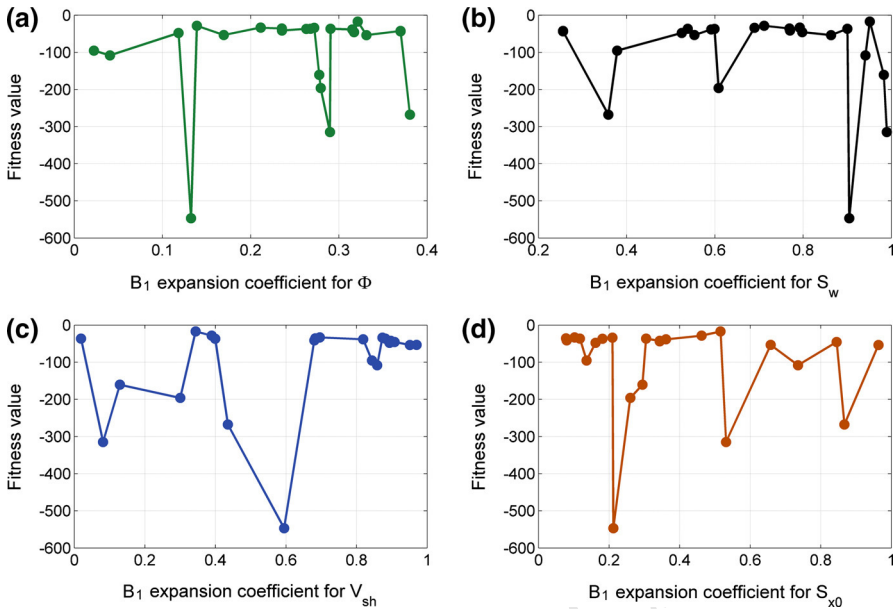


Fig. 3 Fitness values of series expansion coefficients of zeroth degree Legendre polynomials (B_1) contributing the depth function of: **a** porosity (Φ), **b** water saturation in uninvasion zone (S_w), **c** shale volume (V_{sh}), **d** water saturation in invaded zone (S_{x0})

3.2 Testing the Genetic Inversion Method

The FGA-based interval inversion method is applied in well H. For reducing the CPU time of the heuristic search, an approximate solution is given for the petrophysical parameters using Legendre polynomials of 14 degrees in series expansion. In the initialization of the FGA process, the upper and lower limits of expansion coefficients can be chosen within wide limits. The initial values of the expansion coefficients for the zeroth degree Legendre polynomials correspond to the full practical range of petrophysical parameters: $0 \leq B_1^{(\Phi)} \leq 0.4$, $0 \leq B_1^{(S_w)} \leq 1$, $0 \leq B_1^{(S_{x0})} \leq 1$, $0 \leq B_1^{(V_{sh})} \leq 1$. Based on the linear inversion experiments detailed in the previous section, the possible range of higher degree expansion coefficients are set as $-0.2 \leq B_q^{(i)} \leq 0.2$ ($i = 1, 2, 3, 4$ and $q = 1, 2, \dots, 15$). Figure 3 shows that the fitness function defined in Eq. (9) plotted against the coefficients B_1 has several localities. The fitness values at minimum locations correspond to a relative data distance of approximately 800–1000%. The multidimensional fitness function plotted against the expansion coefficients of higher degree Legendre polynomials also has several extrema (Fig. 4), which justifies the use of the FGA method.

A population of 50 individuals is improved by the FGA procedure. When having four petrophysical properties as unknown, the number of expansion coefficients per individual (petrophysical model) is 60 and the total number of genes in the population is 3000. The material balance equation as a constraint is built in the forward problem solution. The FGA search normally takes 10^4 – 10^5 generations to find the global

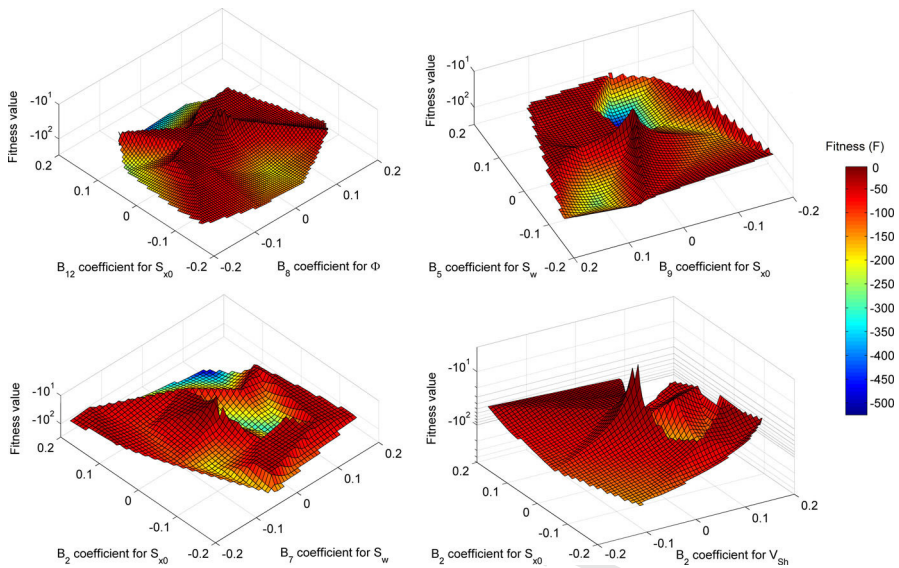


Fig. 4 Fitness functions of two arguments: F is the fitness value inversely related to data misfit, B_q is the series expansion coefficient of the $(q - 1)$ th degree Legendre polynomial as the basis function, porosity (Φ), water saturation in uninvasion zone (S_w), shale volume (V_{sh}), water saturation in invaded zone (S_{x0})

402 optimum in our applications. In contrast, the inversion procedure is run over 5000
 403 iterations to achieve sufficient approximation and requires CPU time of <2 min. The
 404 control parameters of the genetic search are the probability of selecting the best model
 405 ($P_b = 0.03$), the number of crossover retries (100), and the probability of mutation
 406 (0.05). For the reproduction of the best models, the rule of elitism is also applied, by
 407 which the worst individual of the current generation is automatically replaced with the
 408 fittest one of the previous generation. The improvement of the average fitness of the
 409 model population from the initial generation to later generations can be seen in Fig. 5a.
 410 The negative value of the fitness is comparable in order of magnitude with the data
 411 distance defined in Eq. (16). In the initial population, the mean of the fitness is $-7.4 \times$
 412 10^9 ($\sim D_d = 10^9 - 10^{10}\%$), which reduces to -53 at the end of the global optimization
 413 procedure. The best individual has a fitness value of -5.27 , which corresponds to D_d
 414 $= 16.9\%$ relative data distance. The depth variation of the petrophysical parameters
 415 calculated from the estimated expansion coefficients is plotted in Fig. 6.

416 When the degree of Legendre polynomials is not changed in the linearized inversion
 417 (DLSQ) phase (remaining at 14), the data distance does not improve. Better resolution
 418 for the petrophysical model can be reached by increasing the number of expansion
 419 coefficients. By assuming a faster depth variation of petrophysical parameters, in the
 420 DLSQ process, the number of unknowns is increased from 60 to 180 using Legendre
 421 polynomials of degree 44 (Fig. 6). Since the condition number of the self-product
 422 of the Jacobi matrix is $\sim 10^6$, the inverse problem is ill posed. The inverse problem
 423 is regularized by setting a damping factor of 1 for the Marquardt algorithm, which
 424 is decreased to its actual value by 60% in each iteration. The maximal number of

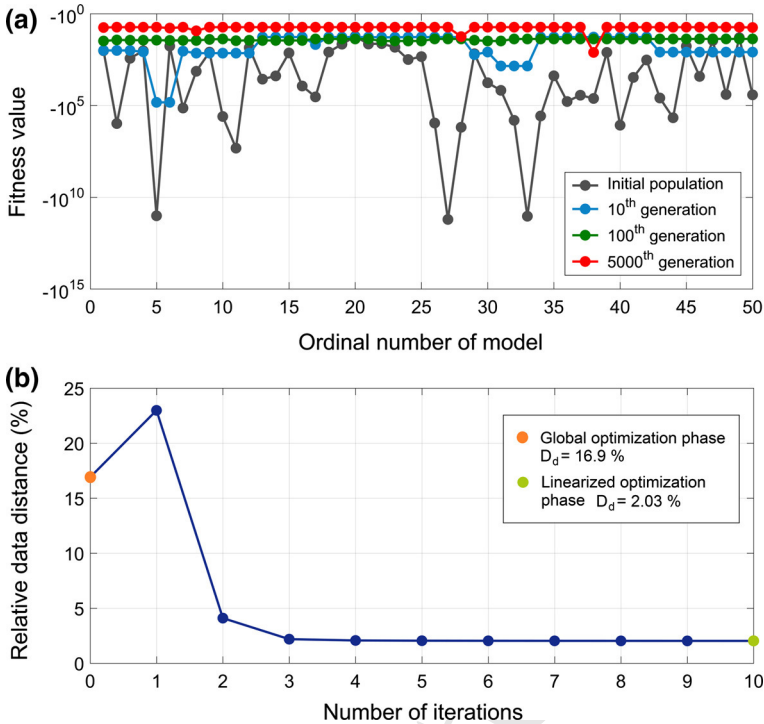


Fig. 5 Genetic interval inversion process including global and linear optimization phases in well H: **a** global inversion result for Legendre polynomials of degree 14, **b** global and linearized inversion result for Legendre polynomials of degree 44. D_d (%) is the relative data distance between the measured and calculated well logs

iterations is 20, at the end of which the regularization factor is 3.6×10^{-5} . The values of both the expansion coefficients and the data distance do not change after ten iterations; thus, Fig. 5b shows the results until that iteration step. The development of convergence is quick and steady. By the increased number of expansion coefficients, the data distance can be effectively decreased. In this case, the inversion procedure stabilizes at relative data distance $D_d = 2.03\%$. It should be noted that, by executing the genetic inversion procedure with initial populations of different sizes, the same optimum is given. The measured well logs are in close agreement with the theoretical logs calculated on the resultant model (see tracks 1–5 in Fig. 7). The fractional volume of water, hydrocarbon, shale, and quartz matrix is plotted in track 6. The irreducible and movable hydrocarbon volumes are directly derived from the inversion results using $V_{hc,mov} = \Phi(S_{x0} - S_w)$ and $V_{hc,irr} = \Phi(1 - S_{x0})$. In the last track of Fig. 7, the pore fluid concentrations are given for unit volume of rock: brine volume (blue color), irreducible hydrocarbon saturation (brown color), and movable hydrocarbon saturation (red color). The petrophysical parameters show strong correlations to those estimated by a linear optimization-based local inversion method (Fig. 8). The result of the regression analysis shows the indication of heteroscedasticity. The non-constant variance in the crossplots may be caused by the different vertical variability of the

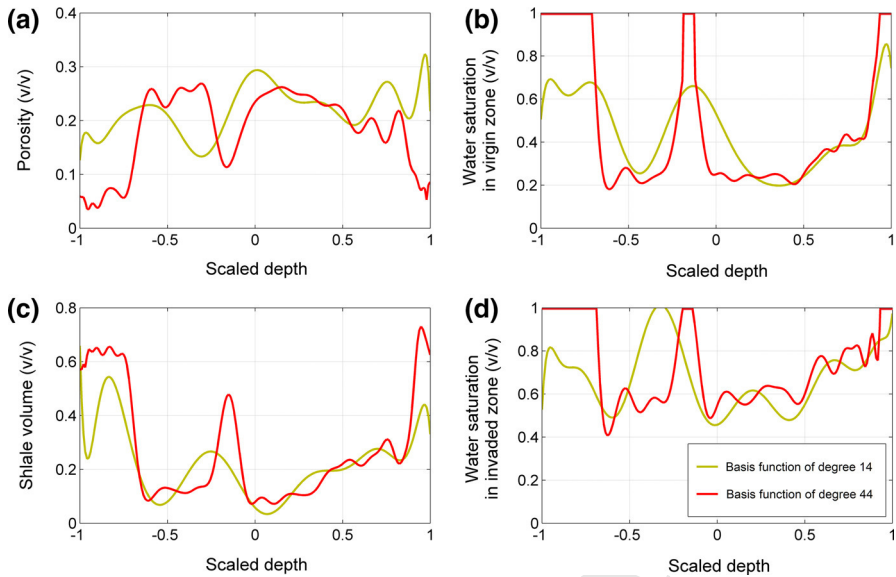


Fig. 6 Petrophysical parameter distributions derived from the series expansion coefficients estimated by the genetic interval inversion procedure in well H: **a** porosity, **b** uninvaded zone water saturation, **c** shale volume, **d** invaded zone water saturation estimated using Legendre polynomials of degree 14 (olive color) and degree 44 (red color)

443 petrophysical parameters described by the same number of series expansion coef-
 444 ficients. The genetic inversion procedure including also the linearized optimization
 445 phase requires a CPU time of 125 s using a quad-core processor workstation. Based
 446 on the inversion experiments, it is concluded that the genetic inversion procedure is
 447 stable and practically independent of the initial model.

448 4 Discussion

449 The feasibility of the linearized interval inversion method was studied previously by
 450 Dobróka et al. (2016). They proved that the estimation accuracy and reliability of
 451 the petrophysical parameters were significantly improved compared to the weighted
 452 least squares-based local inversion method. The results of interval inversion were also
 453 successfully compared to those of robust statistical methods (Szabó et al. 2018). The
 454 application of FGA increases numerical stability and allows the start model to
 455 be provided within broader limits. The linear phase of the hybrid inversion algorithm
 456 gives a possibility of checking the quality and noise sensitivity of the interval inversion
 457 method. After substituting Eq. (13) into Eq. (14), it is seen that the covariance matrix of
 458 observed data is an indispensable input quantity for calculating the estimation accuracy.
 459 In this study, it is assumed that the inverted well logs have different uncertainties, the
 460 values of which are available in sonde specifications, user manuals, or the literature
 461 (Horváth 1973).

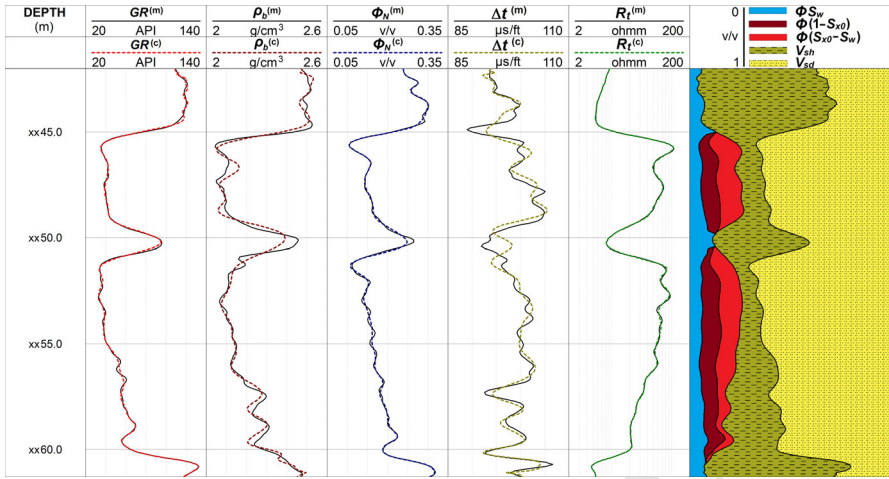


Fig. 7 Results of the genetic inversion procedure in well H: natural gamma ray (GR), density (ρ_b), neutron porosity (Φ_N), acoustic traveltime (Δt), true resistivity (R_t) logs. Superscripts (m) and (c) denote the measured and calculated data, respectively. Estimated petrophysical quantities are porosity (Φ), shale volume (V_{sh}), and water saturations (S_{x0}) and S_w)

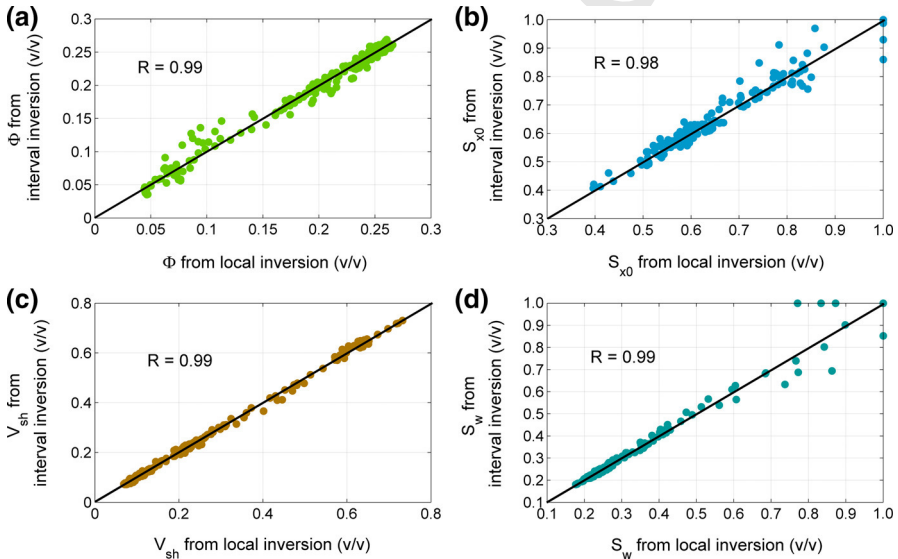


Fig. 8 Regression relation between the results of local inversion and genetic interval inversion in well H. Strong linear connection is indicated for: **a** porosity (Φ), **b** water saturation in uninvasion zone (S_w), **c** shale volume (V_{sh}), **d** water saturation in invasion zone (S_{x0}). R is Pearson's correlation coefficient

462 In order to test the quality of the interval inversion results, the standard deviation
 463 of well logging data are chosen as $\sigma_{GR} = 0.12$, $\sigma_{\rho_b} = 0.08$, $\sigma_{\Phi_N} = 0.13$, $\sigma_{\Delta t} = 0.10$,
 464 and $\sigma_{R_t} = 0.15$, which are even higher than those in Dobróka et al. (2016). At first,
 465 the standard deviation of the expansion coefficients are calculated using Eq. (13). The

466 estimated expansion coefficients including their estimation errors are plotted in Fig. 9a.
 467 The expansion coefficients of the zeroth degree Legendre polynomials are estimated
 468 as $B_1^{(\Phi)} = 0.19$, $B_1^{(S_w)} = 0.50$, $B_1^{(V_{sh})} = 0.27$, and $B_1^{(S_{x0})} = 0.87$, while the values of
 469 higher degrees are represented with an empiric probability density function in Fig. 9b.
 470 As Fig. 9c shows, the estimation error of half of the expansion coefficients is smaller
 471 than 0.05. A maximum around 0.1 is mostly associated to the error of uninverted zone
 472 water saturation, while that of 0.25 can be identified as the error of invaded zone water
 473 saturation. The average correlation of expansion coefficients calculated by Eq. (15) is
 474 $R(\mathbf{B}) = 0.17$, which indicates poorly correlated model parameters and highly reliable
 475 inversion result. Once the variances of expansion coefficients are calculated, one can
 476 derive the estimation error of the petrophysical parameters using Eq. (14). The error
 477 interval of the k th measured variable is calculated as $\Delta d_k (1 \pm \sigma_{d_k})$. The light brown
 478 shaded area in Fig. 10a shows the error intervals calculated from data variances. Tracks
 479 1–4 of Fig. 10b show the estimation error of the petrophysical properties with olive
 480 color shaded area, the average values of which for the entire processing interval are
 481 given as $\bar{\sigma}_\Phi = 0.03 \text{ v/v}$, $\bar{\sigma}_{S_w} = 2.6 \text{ v/v}$, $\bar{\sigma}_{V_{sh}} = 0.16 \text{ v/v}$, and $\bar{\sigma}_{S_{x0}} = 11.7 \text{ v/v}$.
 482 The correlation between the petrophysical parameters is moderate (see track 5), the
 483 average being $R(\mathbf{m}) = 0.38$ (for local inversion, it is 0.59 in well H). From the standard
 484 deviations and Pearson's correlation coefficients, it is concluded that the porosity
 485 and shale volume are estimated more accurately than the water saturation in both
 486 the invaded and virgin zones. The latter two are more strongly correlated to each
 487 other than the previous ones, since the depth averages are $\overline{\text{corr}}(\Phi, V_{sh}) = 0.19$ and
 488 $\overline{\text{corr}}(S_w, S_{x0}) = 0.74$. The strong correlation between the water saturations causes
 489 relatively lower estimation accuracy for them. High correlation coefficients always
 490 result in the problem of ambiguity. The root of this problem is found in the structure
 491 of sonde response equations, which can be improved by revising the solution of the
 492 forward problem. From the point of view of inverse modeling, highly correlated model
 493 parameters should be estimated outside the inversion procedure. In conclusion, the
 494 advantage of the combined interval inversion approach is that it gives more accurate
 495 results than those of the marginally overdetermined local inversion.

496 The optimal number of basis functions can be found by seeking the minimum of
 497 the average correlation between the estimated expansion coefficients (Dobróka et al.
 498 2016). For the combined interval inversion method, the dependency of the inversion
 499 result on the degree of the Legendre polynomials must be checked. By using the same
 500 well-logging data set and parameter settings, the inversion process is run by different
 501 numbers of basis functions selected between 1 and 44 in the genetic algorithm phase.
 502 The blue dots in Fig. 11a show that the interval inversion procedure combining the
 503 FGA and the DLSQ method always give the same optimum. In the genetic inversion
 504 phase, the relative data distance decreases significantly up to 16 basis functions. Fur-
 505 ther improvement can only be achieved by increasing the number of generations, which
 506 is currently 5000 steps for each inversion experimental run. Thus, in the case study,
 507 Legendre polynomials of 14 degrees in series expansion were chosen. The advantage
 508 of using a relatively small number of basis functions is the low computational cost
 509 and high estimation accuracy. As shown in Fig. 11b, the CPU time nonlinearly and
 510 highly increases with the number of polynomials. In Fig. 12, one can observe how the

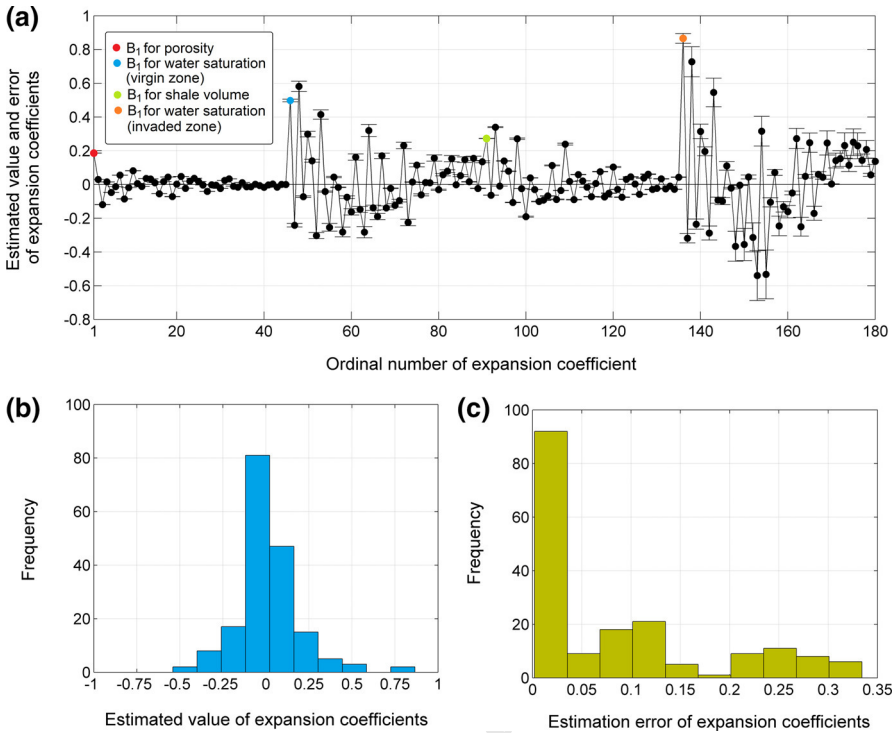


Fig. 9 Series expansion coefficients including their error bars estimated by genetic inversion in well H (a); histogram of the estimated expansion coefficients (b); histogram of the standard deviation of expansion coefficients (c)

511 FGA approximates the result of the combined interval inversion procedure (FGA +
 512 DLSQ) when using different numbers of basis functions. These tests reveal that the
 513 FGA provides a proper starting model for the DLSQ inversion, which gives stable
 514 predictions for different numbers of basis functions (Fig. 11a). In contrast, a single
 515 linearized inversion (DLSQ) can be highly affected by the starting model (Fig. 2).
 516 The difference between the results of the single and combined interval inversion
 517 procedures is explained as: (1) the data distance calculated for the starting models is
 518 around 100% or higher for the cases shown in Fig. 2, while in the case of using a
 519 fast FGA step, it is no more than 40%, as shown in Fig. 11a (i.e., the initial model is
 520 closer to the optimum); (2) the series expansion coefficients of higher order Legendre
 521 polynomials are set to zero (i.e., homogeneous starting model is assumed) before the
 522 DLSQ inversion in all examples of Fig. 2, whereas in the frame of the FGA + DLSQ
 523 procedure, the same coefficients are estimated first by FGA to give a more sophis-
 524 ticated (inhomogeneous) initial model for DLSQ inversion (Fig. 12). The estimated
 525 (non-zero) values of the expansion coefficients of these starting models are just further
 526 refined by DLSQ inversion, which brings stability to the combined interval inversion
 527 procedure. The above tests show that a trade-off should be made between the number
 528 of expansion coefficients as unknowns of the inverse problem (i.e., vertical resolution
 529 of petrophysical properties) and total CPU time.

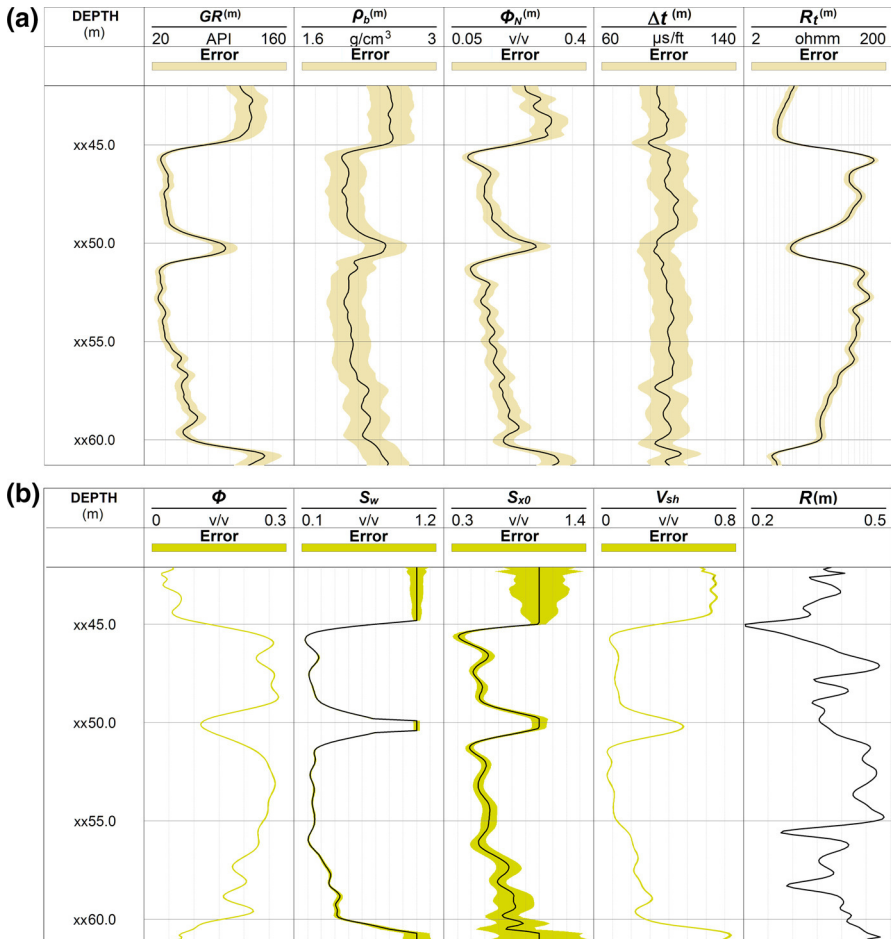


Fig. 10 Quality check of the interval inversion procedure in well H: observed natural gamma ray (GR), density (ρ_b), neutron porosity (Φ_N), acoustic traveltime (Δt), true resistivity (R_t) logs with accuracy ranges (a); inversion results with estimation errors: porosity (Φ), shale volume (V_{sh}), invaded and uninvaded zone water saturation (S_{x0} and S_w)

530 The feasibility of the combined interval inversion method can be further proven
 531 by making synthetic inversion experiments. Well logs are calculated by Eqs. (1)–(5)
 532 using a known petrophysical model. The depth variations of petrophysical proper-
 533 ties of a hydrocarbon-saturated shaly-sand formation are constructed as 24 degree
 534 Legendre polynomials. To simulate real borehole measurements, different amounts of
 535 random noise can be added to the synthetic data. The k th noisy data at a given depth
 536 is calculated as $d'_k = d_k (1 + N(\mu, \sigma))$, where $\mu = 0$ is the expected value and σ is
 537 the standard deviation of the desired noise level. The control parameters and iteration
 538 number of the genetic inversion process are chosen similarly as in Sect. 3.2. The zone
 539 parameters of the tool response equations are given in Table 1. The number of Leg-
 540 endre polynomials in Eq. (7) is chosen as 24 in both the genetic and linear phases.

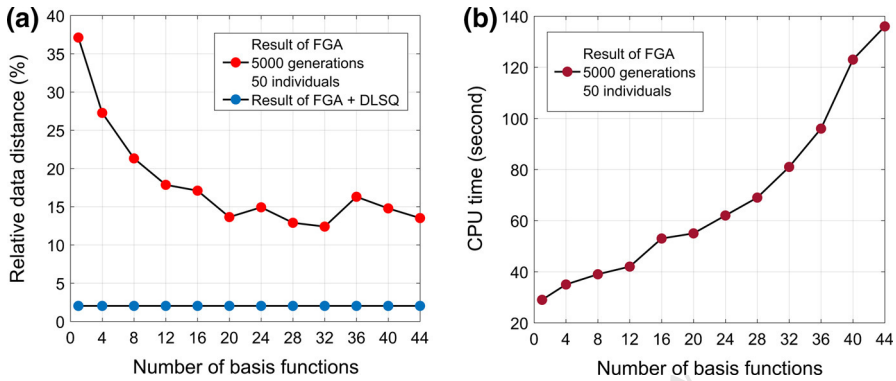


Fig. 11 Relative data distance versus the number of basis functions used in the genetic inversion phase of the combined interval inversion procedure (a); the CPU time requirement for the genetic algorithm versus the number of basis functions (b)

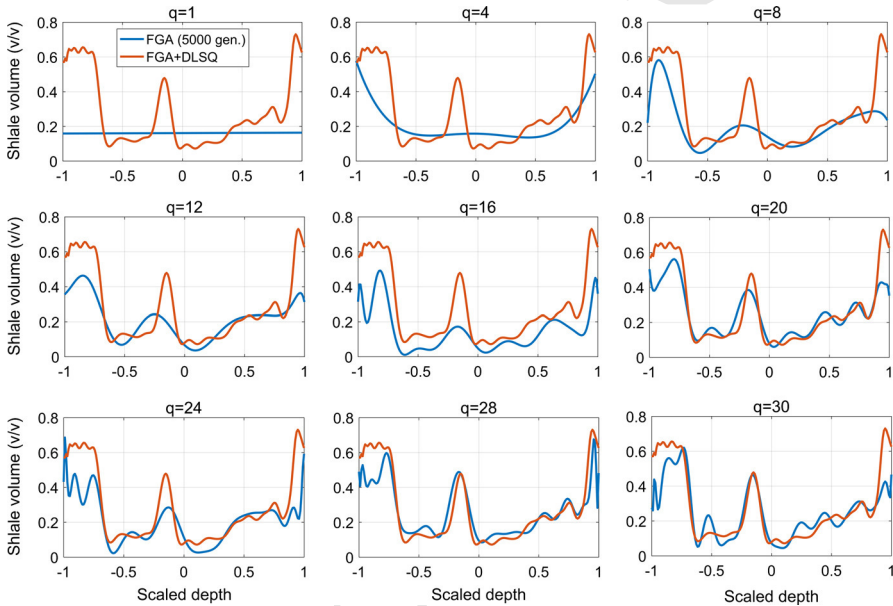


Fig. 12 Inversion results for different numbers of basis functions (q). The blue curves represent the results of genetic inversion using 5000 generations and the red curves show the results of the combined interval inversion procedure

541 The inversion results using a synthetic data set contaminated by 4% Gaussian noise is
 542 included in Fig. 13. The relative data distance between the noisy and calculated data
 543 is $D_d = 4.09\%$, which is proportional to the noise level of the input data (Fig. 13a).
 544 The petrophysical parameters of the true model can be directly compared to those
 545 of the predicted model in Fig. 13b. The GR image (track 1) shows the change of
 546 lithology, tracks 2 and 4 illustrate the saturation curves, while tracks 3 and 5 represent
 547 the results of compositional analysis. The overdetermination ratio of 12.5 results in

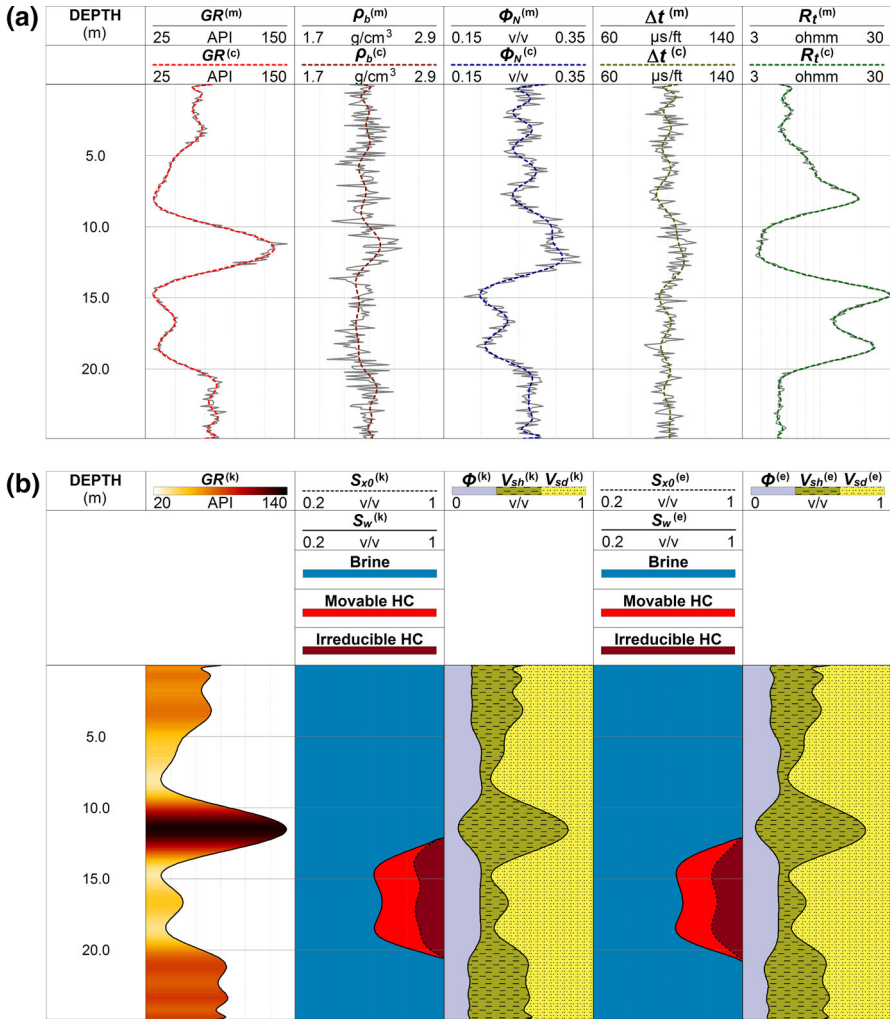


Fig. 13 Results of the combined interval inversion method using synthetic data contaminated with 4% Gaussian noise. Well logs of quasi measured data (m) and those of calculated data (c) on the estimated model (a); parameters of the known (k) model and estimated (e) model (b); porosity (Φ), water saturation in uninvaded zone (S_w) and in invaded zone (S_{x0}), and shale volume (V_{sh})

548 highly accurate estimation results. Assuming the data uncertainties given in the case
 549 study, the average estimation errors of petrophysical properties for the entire process-
 550 ing interval are obtained as $\bar{\sigma}_\Phi = 0.03$ v/v, $\bar{\sigma}_{S_w} = 2.3$ v/v, $\bar{\sigma}_{V_{sh}} = 0.14$ v/v, and
 551 $\bar{\sigma}_{S_{x0}} = 3.3$ v/v, which show nearly the same (slightly better) results as those of the
 552 field case. The average correlation between the series expansion coefficients is $R(\mathbf{B}) =$
 553 0.09 , which indicates practically uncorrelated model parameters and highly reliable
 554 inversion result. The CPU time requirement of the inversion run is approximately
 555 2 min.

5 Conclusions

A float-encoded genetic algorithm (FGA)-based interval inversion method is suggested to evaluate the petrophysical properties of inhomogeneous hydrocarbon formations. The global inversion approach implemented to solve the problem of interval inversion makes the inversion procedure computationally more effective and stable than linearized techniques. The feasibility is demonstrated in a gas-bearing shaly-sand formation and the results are compared to those of independent local inversion.

It is shown that the genetic inversion method is derivative-free and initial model-independent, including a quick forward problem solution. The coupled linear phase allows the fast calculation of the final solution, including the estimation error of both the series expansion coefficients and petrophysical parameters. The high rate of over-determination originally ensures a low noise sensitivity; moreover, the FGA improves the fit between the measured and calculated data. For describing the geological structure, the basis functions in series expansion can be chosen arbitrarily. By selecting the number of expansion coefficients, one can control the CPU time of the inversion process, estimation accuracy, and the vertical resolution of the petrophysical model. Within reasonable limits, the genetic inversion procedure allows the integration of more well logs types and bigger data sets. This may require not only the development of new response functions or sophisticated forward modeling algorithms, but also the definition of the zone parameters from an objective source. The latter can be efficiently performed within the interval inversion procedure, which can be solved effectively by the interval inversion approach. The automated estimation of zone parameters sets a new perspective in well log analysis, which does not require prior knowledge of zone parameters for the inversion procedure. While preserving its stability, the efficiency of the interval inversion method can be increased by estimating some volumetric petrophysical parameters outside the inversion procedure. For instance, multivariate statistical techniques, like factor analysis, can be used to estimate the shale volume or other critical unknowns from an independent source. The resultant parameters can then be fixed during the interval inversion procedure. This may further increase the estimation accuracy for the remaining inversion unknowns.

The series expansion-based inversion methodology can be extended to cross-hole applications. By using Legendre polynomials of two or three variables as basis functions, the petrophysical parameters and the lateral (and, of course, the vertical) change of layer boundaries can be simultaneously estimated. In order to perform an initial model-independent two- or three-dimensional interval inversion of multi-borehole data, the genetic inversion method is preferably applied. In the future, the suggested genetic inversion workflow will be tested for the evaluation of unconventional hydrocarbon reservoirs, where the interval inversion method may be successfully applied for estimating an increasing number of unknowns due to multi-mineral rock matrix, organic content, and complex pore-space and fluid-saturation conditions.

Acknowledgements This research was supported by the GINOP-2.3.2-15-2016-00010 “Development of enhanced engineering methods with the aim at utilization of subterranean energy resources” project in the framework of the Széchenyi 2020 Plan, funded by the European Union, co-financed by the European Structural and Investment Funds. The first author is thankful for the support of the above GINOP project.

600 **References**

- 601 Alberty M, Hashmy K (1984) Application of ULTRA to log analysis. In: SPWLA symposium transactions.
602 Paper Z, pp 1–17
- 603 Aleardi M (2015) Seismic velocity estimation from well log data with genetic algorithms in comparison to
604 neural networks and multilinear approaches. *J Appl Geophys* 117:13–22
- 605 Aleardi M, Mazzotti A (2017) 1D elastic full-waveform inversion and uncertainty estimation by means of
606 a hybrid genetic algorithm–Gibbs sampler approach. *Geophys Prospect* 65:64–85
- 607 Ali Ahmadi M, Zendehboudi S, Lohi A, Elkamel A, Chatzis I (2013) Reservoir permeability prediction by
608 neural networks combined with hybrid genetic algorithm and particle swarm optimization. *Geophys*
609 *Prospect* 61:582–598
- 610 Archie GE (1942) The electrical resistivity log as an aid in determining some reservoir characteristics. *SPE*
611 *Trans AIME* 146:54–62
- 612 Baker Atlas (1996) OPTIMA, eXpress reference manual. Baker Atlas, Western Atlas International, Inc.,
613 Houston
- 614 Ball SM, Chace DM, Fertl WH (1987) The Well Data System (WDS): an advanced formation evaluation
615 concept in a microcomputer environment. In: Proceedings of the SPE eastern regional meeting, paper
616 17034, pp 61–85
- 617 Chunduru RK, Sen MK, Stoffa PL (1997) Hybrid optimization methods for geophysical inversion. *Geo-*
618 *physics* 62:1196–1207
- 619 Cranganu C, Luchian H, Breaban ME (2015) Artificial intelligent approaches in petroleum geosciences.
620 Springer, Berlin
- 621 Dobróka M, Szabó NP (2011) Interval inversion of well-logging data for objective determination of textural
622 parameters. *Acta Geophys* 59:907–934
- 623 Dobróka M, Szabó NP (2012) Interval inversion of well-logging data for automatic determination of for-
624 mation boundaries by using a float-encoded genetic algorithm. *J Pet Sci Eng* 86–87:144–152
- 625 Dobróka M, Szabó PN, Cardarelli E, Vass P (2009) 2D inversion of borehole logging data for simultaneous
626 determination of rock interfaces and petrophysical parameters. *Acta Geod Geophys Hung* 44:459–479
- 627 Dobróka M, Szabó NP, Turai E (2012) Interval inversion of borehole data for petrophysical characterization
628 of complex reservoirs. *Acta Geod Geophys Hung* 47:172–184
- 629 Dobróka M, Szabó NP, Tóth J, Vass P (2016) Interval inversion approach for an improved interpretation of
630 well logs. *Geophysics* 81:D155–D167
- 631 Dorrington KP, Link CA (2004) Genetic-algorithm/neural-network approach to seismic attribute selection
632 for well-log prediction. *Geophysics* 69:212–221
- 633 Drahos D (2005) Inversion of engineering geophysical penetration sounding logs measured along a profile.
634 *Acta Geod Geophys Hung* 40:193–202
- 635 Eidsvik J, Mukerji T, Switzer P (2004) Estimation of geological attributes from a well log: an application
636 of hidden Markov chains. *Math Geol* 36:379–397
- 637 Gajda-Zagórska E, Schaefer R, Smółka M, Paszyński M, Pardo D (2015) A hybrid method for inversion of
638 3D DC resistivity logging measurements. *Nat Comput* 14:355–374
- 639 Galsa A, Herein M, Drahos D, Herein A (2016) Effect of the eccentricity of normal resistivity borehole
640 tools on the current field and resistivity measurement. *J Appl Geophys* 134:281–290
- 641 Holland JH (1975) *Adaptation in natural and artificial systems*. University of Michigan Press, Ann Arbor
- 642 Horváth SB (1973) The accuracy of petrophysical parameters as derived by computer processing. *Log Anal*
643 14:16–33
- 644 Houck CR, Joines JA, Kay MG (1995) A genetic algorithm for function optimization: a Matlab implemen-
645 tation. NCSU-IE technical report 95-09, North Carolina State University, pp 1–14
- 646 Jarzyna JA, Cichy A, Drahos D, Galsa A, Bała MJ, Ossowski A (2016) New methods for modeling laterolog
647 resistivity corrections. *Acta Geophys* 64:417–442
- 648 Lindberg DV, Grana D (2015) Petro-elastic log-facies classification using the expectation–maximization
649 algorithm and hidden Markov models. *Math Geosci* 47:719–752
- 650 Malkoti A, Vedanti N, Bhattacharya AK (2017) Inversion of well log data using improved shale model for
651 determination of petrophysical parameters. *J Indian Geophys Union* 21:96–104
- 652 Marquardt DW (1959) Solution of nonlinear chemical engineering models. *Chem Eng Prog* 55:65–70
- 653 Mayer C, Sibbit AM (1980) GLOBAL, a new approach to computer-processed log interpretation. In:
654 Proceedings of the 55th SPE annual fall technical conference and exhibition, paper 9341, pp 1–14
- 655 Menke W (1984) *Geophysical data analysis: discrete inverse theory*. Academic Press, Cambridge

- 656 Michalewicz Z (1992) Genetic algorithms + data structures = evolution programs. Springer, Berlin
657 Mundim KC, Lemaire TJ, Bassrei A (1998) Optimization of non-linear gravity models through generalized
658 simulated annealing. *Physica A* 252:405–416
- 659 Narayan JP, Yadav L (2006) Application of adaptive processing technique for the inversion of open hole
660 logs recorded in oil fields of Indian basins. In: Proceedings of the SPG 6th international conference
661 and exposition on petroleum geophysics, pp 505–512
- 662 Sambridge M (1999) Geophysical inversion with a neighbourhood algorithm—I. Searching a parameter
663 space. *Geophys J Int* 138:479–494
- 664 Sambridge M, Drijkoningen G (1992) Genetic algorithms in seismic waveform inversion. *Geophys J Int*
665 109:323–342
- 666 Schlumberger (1989) Log interpretation principles/applications. Seventh printing. Schlumberger, Houston
667 Sen MK, Stoffa PL (1995) Global optimization methods in geophysical inversion. Elsevier, Amsterdam
- 668 Szabó NP (2004) Global inversion of well log data. *Geophys Trans* 44:313–329
- 669 Szabó NP (2016) Hydrocarbon formation evaluation using an efficient genetic algorithm-based factor anal-
670 ysis method. In: Proceedings of the 15th European conference on the mathematics of oil recovery,
671 paper Mo P071, pp 1–12
- 672 Szabó NP, Dobróka M (2013) Extending the application of a shale volume estimation formula derived from
673 factor analysis of wireline logging data. *Math Geosci* 45:837–850
- 674 Szabó NP, Dobróka M (2018) Exploratory factor analysis of wireline logs using a float-encoded genetic
675 algorithm. *Math Geosci* 50:317–335
- 676 Szabó NP, Balogh GP, Stickle J (2018) Most frequent value-based factor analysis of direct-push logging
677 data. *Geophys Prospect* 66:530–548
- 678 Szijártó M, Balázs L, Drahos D, Galsa A (2017) Numerical sensitivity test of three-electrode laterolog
679 borehole tool. *Acta Geophys* 65:701–712
- 680 Szűcs P, Civan F (1996) Multi-layer well log interpretation using the simulated annealing method. *J Pet Sci*
681 *Eng* 14:209–220
- 682 Tarantola A (2005) Inverse problem theory and methods for model parameter estimation. Society of Indus-
683 trial and Applied Mathematics (SIAM), Philadelphia
- 684 Tlas M, Asfahani J (2008) Using of the adaptive simulated annealing (ASA) for quantitative interpretation
685 of self-potential anomalies due to simple geometrical structures. *J King Abdulaziz Univ Earth Sci*
686 19:99–118
- 687 Toushmalani R (2013) Comparison result of inversion of gravity data of a fault by particle swarm optimiza-
688 tion and Levenberg–Marquardt methods. *SpringerPlus* 2:462
- 689 Woznicka U, Jarzyna J, Cichy A (2009) Forward modelling and inverse problem in the comprehensive
690 interpretation of well logs. *Geophys Prospect* 57:99–109
- 691 Wyllie MRJ, Gregory AR, Gardner LW (1956) Elastic wave velocities in heterogeneous and porous media.
692 *Geophysics* 21:41–70
- 693 Yang XS (2013) Metaheuristic algorithms for inverse problems. *Int J Innov Comput Appl* 5:76–84